

Computational modelling of the collective stochastic motion of Kinesin nano motors

Yousef Jamali ¹, M. Ebrahim Foulaadvand ^{1,2} and H. Rafii Tabar ¹

¹ Computational Physical Sciences Research Laboratory, Department of Nano-Science, Institute for Research in Fundamental Sciences (IPM), P.O. Box 19395-5531, Tehran, Iran.

² Department of Physics, Zanjan University, P.O. Box 45196-313, Zanjan, Iran.

We have developed a two dimensional stochastic molecular dynamics model for the description of intra cellular collective motion of bio motors, in particular Kinesins, on a microtubular track. The model is capable of reproducing the hand-over-hand mechanism of the directed motion along the microtubule. The model gives the average directed velocity and the current of Kinesins along the microtubule. It is shown that beyond a certain density of Kinesins, the average velocity and current undergo notable decrease which is due to formation of traffic jams in the system.

I. INTRODUCTION

Various complex functions of Eucariotic cells namely mitosis, intracellular transports and cell motility are based on the cooperative motion of molecular motor proteins such as Dyneins, Kinesins and Myosins [1, 2, 3, 4]. These molecular motors move on cytoskeletal filaments like microtubules and F-actins. The mentioned phenomena exhibit a variety of self-organized processes and patterns which are characterized by their time scales [5, 6, 7, 8, 9]. A large number of in-vitro experiments have revealed that the motion of Kinesin is *processive* i.e., it performs stroke-type steps on its track before detachment [10, 11, 12]. It is now well established that the Kinesins motion is derived by the free energy released in the chemical hydrolysis reaction of ATP (adenosine-triphosphate). The fuel of the motion that is the ATP molecules arrive randomly in the vicinity of Kinesins. Consequently, the directed motion takes place on a stochastic grounds. During each step in which one period of the microtubule, hereafter referred to as MT, is covered, one ATP molecule is hydrolysed. The underlying mechanism responsible for this forward motion is partially understood. Two basic mechanisms have been proposed. In the first one the so-called *inchworm mechanism*, one head of Kinesin drag the other one which is always at the rear [13]. In this mechanism, there is an asymmetry between the lagging. The second mechanism which is called *hand-over-hand* has much resemblance to human walking. This mechanism involves repeated docking and undocking of both heads upon breaking of the chemical bond with the MT in the course of ATP hydrolysis [14, 15]. At each stepping event, the rear head executes a forward motion of 16 nm and attaches to the tubulin binding site ahead of the front head. Recent empirical evidences overwhelmingly have established that hand-over-hand mechanism is the true mechanism [14]. In recent years various approaches have been proposed to model the directed motion of nano-sized bio motors. Simple random walk was used as a simple though efficient framework for modelling such kind of motion [16, 17, 18, 19]. In this framework, Kinesins are assumed to be point particles which execute a directed random walk on a discrete one dimensional filament, as a model

for microtubular track, with lattice spacing equal to Kinesin walking distance i.e. 8 nm. Due to stochasticity in the Kinesin motion, it would be reasonable to incorporate degrees of randomness in the modelling approach. In this spirit, a new approach namely asymmetric particle hopping models in continuous time which are based on master equation approach came into play [17, 20, 21, 22]. Another theoretical approach for the modelling of bio motors motion is the *so-called* ratchet mechanism [4]. In this mechanism, the directed motion is generated by a time-dependent periodic potential which is switched between two states [23, 24, 25, 26, 27, 28, 29, 30]. The stochasticity comes in the manner in which the potential switches from one state to the other one and reflects the random arrival of ATP molecules and conformational transitions which changes the interacting potential between Kinesin and MT. In principle, more than one Kinesins can simultaneously move on a single MT. Kinesins do certainly interact with each other. While the true interaction potential between adjacent Kinesins has not yet empirically explored, in-vitro observations have revealed the collective motion of Kinesins which arises from the interaction between these motors [31]. In order to find some insight into the nature of the Kinesins motion, we have developed a Langevin-type model which incorporates interaction among Kinesins. Our aim is to improve our understanding on the spatio-temporal organisations of intra cellular transport phenomena and find the mechanism responsible for formation of molecular traffic jams.

II. MODELLING OF KINESINS MOVEMENT

The model we have considered is a generalisation of the model proposed in [30] for the motion of a single Kinesin.

We shall now explain our stochastic ratchet model in some details. The force acting on each Kinesin head consists of four terms as follows:

$$\mathbf{F} = -\vec{\nabla}H_{ratchet} - \vec{\nabla}H_{bistable} - \vec{\nabla}H_{rep}(\Delta r) + \Gamma. \quad (1)$$

$H_{ratchet}$ is the stochastic ratchet potential which models the interaction between Kinesin and microtubule. $H_{bistable}$ is a bistable potential that models the elastic

coupling between two heads of Kinesin, H_{rep} is the repulsive potential between adjacent Kinesins and finally Γ represents both the stochastic Brownian and the frictional forces experienced by Kinesin heads due to thermal noise in the intra cellular environment. Let us explain these four terms in more details.

A. Ratchet potential

The ratchet potential $H(x, y, t)$ should involve an asymmetry along the MT. More precisely, we have taken the form of ratchet potential as follows [30]:

$$H(x, y, t) = CH_x(x)H_y(y)A(t)S(t) \quad (2)$$

With periodicity in x direction i.e., $H(x + L, y, t) = H(x, y, t)$ where L is the microtubule period which is about 8 nm . For $H_x(x)$ we have used the first eleven terms of a Fourier series of an asymmetric function $W(x)$ as follows:

$$H_x(x) = a_0 + \sum_{m=1}^5 a_m \cos\left(\frac{2\pi mx}{L}\right) + b_m \sin\left(\frac{2\pi mx}{L}\right) \quad (3)$$

The coefficients a_0, a_m and b_m $m = 1, \dots, 5$ are Fourier coefficients. For the asymmetric function $W(x)$ we chose the saw-tooth function:

$$W(x) = \frac{10}{9}\left(\frac{x}{L} - \left[\frac{x}{L}\right]\right) \quad \frac{x}{L} - \left[\frac{x}{L}\right] < 0.9$$

$$W(x) = 10\left(\frac{x}{L} - \left[\frac{x}{L}\right]\right) - 10 \quad \frac{x}{L} - \left[\frac{x}{L}\right] > 0.9 \quad (4)$$

Where $[]$ denotes the integer part. The summation form of $H_x(x)$ has been used for computational convenience. Figure (1) shows $H_x(x)$ versus x .

Each peak of $H_x(x)$ is located at a distance $0.1L$ from the position of the next minimum. For more details see Ref. [30]. Concerning the part of potential $H_y(y)$ responsible for the perpendicular direction to the MT we have used the following potential :

$$H_y(y) = -\frac{1}{y^2 + y_0^2} \quad (5)$$

where $y_0 = 0.1\sqrt{L}$. It is assumed that the above form of $H_y(y)$ can model the interaction between the molecules making up the Kinesin head and the MT. The symmetry of the function allows for detaching both in upward and downward directions perpendicular to the MT. This function is smoother than the Morse potential therefore

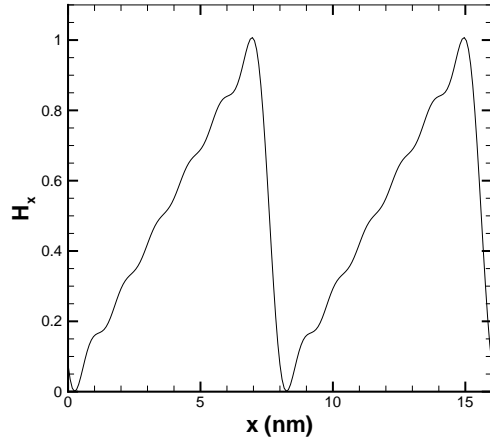


FIG. 1: Periodic dependence of H_x on x .

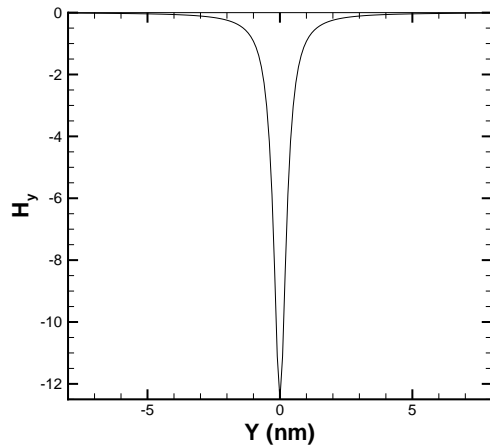


FIG. 2: Dependence of H_y on the perpendicular direction y .

we can choose larger time steps which can speed up the simulation. Figure (2) shows H_y .

Now we shall discuss the time dependent terms i.e., $A(t)$ and $S(t)$ of the Ratchet potential. The stochastic variable $A(t)$ specifies the biochemical affinity of each Kinesin head. It is a flashing potential which can switch between two discrete values $A(t) = 0, 1$. The value of $A(t)$ depends on the biochemical status of the ATPase binding site of the head. The biochemical cycle is divided into four status.[14, 32, 33] In the first status, denoted by K, the ATPase binding site contains no ATP molecule. When an ATP molecules arrives at the binding site, the head is said to be in its second status which is denoted by K.ATP. The third status is associated with the hydrolysis of the absorbed ATP into ADP plus an inorganic phosphate molecule Pi. This status is denoted by K.ADP.Pi. Eventually after releasing the Pi molecule, the head is characterized by its fourth status K.ADP. The biochemi-

cal cycle is accomplished by releasing the ADP molecule. In the status 1-3 the head has a high affinity ($A = 1$) to attach, or to keep its attached condition to the MT. On the other hand, in the fourth status i.e., K.ADP the affinity will considerably reduced ($A = 0$) due to some conformational changes. The second term $S(t)$ is related to the interaction between Kinesins. Besides biochemical status, each head can be either attached to the MT or detached from it. Each head can attach only to particular sites on the MT. Since only one head can attach to each MT binding site, the potential seen by each head depends on the occupancy of its adjacent MT binding site. For adjacent Kinesins to MT, the stochastic variable $S(t)$ describes the occupancy of the corresponding nearest binding site on the MT. It is zero if this site is already occupied by another head and one otherwise (see Fig.4). Parameter C is set at $C = 0.01 \text{ eV}$. The value of constant C determines the depth of the potential well. Its size must be such that the energy difference between the on-state ($A=1$) and the off-state ($A=0$) under the equilibrium condition is comparable with the energy released from the hydrolysis of the ATP i.e.,

$$[H(x, y, t)]_{A(t)=1} - [H(x, y, t)]_{A(t)=0} \leq E_{ATP \rightarrow ADP + Pi} \quad (6)$$

B. Viscous and stochastic thermal noise terms

The force Γ , which for simplicity acts in two dimension, has the following structure:

$$\Gamma_x = -\eta\dot{x}(t) + \xi_x(t). \quad (7)$$

$$\Gamma_y = -\eta\dot{y}(t) + \xi_y(t). \quad (8)$$

The first term corresponds to energy dissipation due to viscosity of the surrounding fluid. ξ_x and ξ_y are stationary random Gaussian white noises with zero mean. More precisely we have:

$$\langle \xi_i(t)\xi_j(t') \rangle = 2\eta k_B T \delta(t-t')\delta_{ij} \quad (9)$$

The drag coefficient η for a Kinesin in an aqueous environment is reported at $\eta \approx 6 \times 10^{-8} \text{ pNs/nm}$ [24]. We have taken this value for η in this paper.

C. The bistable potential

The bistable potential is responsible for the elastic coupling of the two Kinesin heads. This potential is expressed by the following form [29, 30]:

$$H_{bistable}(\Delta r) = C_1 \left[1 + \left(\frac{\Delta r}{l} \right)^4 - 2 \left(\frac{\Delta r}{l} \right)^2 \right] \quad (10)$$

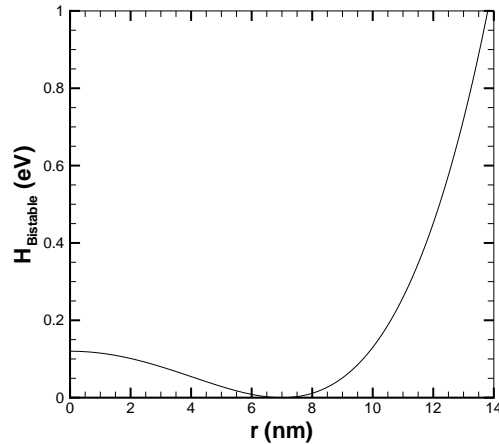


FIG. 3: Bistable potential between two heads vs distance. It models the elastic interaction between Kinesin heads.

In which Δr is the distance between the two heads, $C_1 = 0.12 \text{ eV}$ is the amplitude of the potential and represents the coupling strength between heads, and $l = 0.7L$ is the distance between the two potential minima. In the following figure, we have sketched the dependence of the bistable potential versus distance.

D. The potential between different Kinesins heads

In order to model the interaction between adjacent Kinesins, we introduce a short-ranged repulsive potential between heads of different Kinesins. More concisely, we have used the shifted-force repulsive part of the Lennard-Jones potential as follows:

$$H_{rep}(\Delta r) = U(\Delta r) - U(\Delta r_c) \quad (11)$$

In which $U(\Delta r) = \epsilon \left(\frac{\sigma}{r} \right)^6$ with $\epsilon = 0.2 \text{ eV}$, $\sigma = 70 \text{ A}^0$ and the cut off length $r_c = 80 \text{ A}^0$. This repulsive potential prevents the heads of adjacent Kinesins from getting too close to each other.

E. simulation details

We have not yet discussed in details how quantities A and S vary with time. To this end, we introduce a quantity $a(t)$ for each Kinesin's head which specifies whether at time t the head is attached to the MT or not. $a(t)$ is one if the head is attached to a binding site and zero otherwise. Before proceeding further let us specify when we consider a head attached to a MT binding site. If at any time step, a head has a high affinity ($A(t) = 1$) and is located within a rectangular box with size $\delta_x = 3.8 \text{ nm}$ and $\delta_y = 0.8 \text{ nm}$ centred at a binding site of the MT then we consider this head as an attached one.

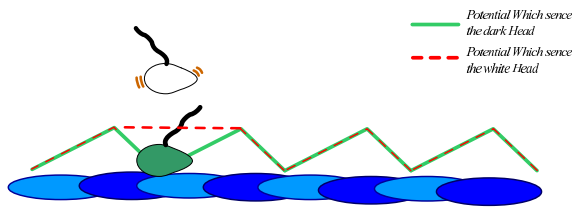


FIG. 4: For adjacent heads to MT, The ratchet potential is zero if the nearest binding site on the MT is already occupied by another head. A head is considered attached to a binding site if it is in a small vicinity of that site.

Not we turn into $A(t)$. Apparently the biochemical cycles of each head can be described by transition rates from one state to the other one. We assume that the average time that each head spends in the states K, K.ATP or K.ADP.Pi is in the order of ms when the head is attached to the MT [34, 35]. We note that this average time depend on the attachment of the head and the position of its partner head. The average time a head spends in the fourth state K.ADP is much shorter and is in the order of μs [34, 36]. Since the rate of ATP consumption is considerably reduced when a head is detached [37, 38, 39], in our model we have assumed that only an attached head received an ATP molecule. Moreover, we experimentally know the rate at which an attached head makes a transition from the state $K \rightarrow K.ATP$ strongly depends on the attaching state and position of its partner head [39, 40]. In case the partner head is attached and rear, the above rate is lowered about two orders of magnitude. We have tuned the corresponding rates in our code such that the processivity and the average velocity of a single Kinesin coincides with the known empirical findings. Consequently, we used these adjusted rates in the collective motion of Kinesins. Periodic boundary condition have been imposed and the Kinesins motion are assumed, for simplicity, to be restricted to two dimension along x and y axes. The size of the simulation box was taken as follows: $L_x = 50 L$, $L_y = 40 L$. The MT is located along the x - axis at $y = 0$ and $y \in [-\frac{L_y}{2}, \frac{L_y}{2}]$. Time step δt was set to $5 \times 10^{-10} s$. The system has been simulated for 3×10^{10} timesteps in each run. The first 5×10^9 timesteps are discarded for reaching to equilibrium. Kinesin global density ρ_g is defined as the number of Kinesins per binding site of the MT. Certainly ρ_g can exceed one.

III. SIMULATION RESULTS

Generically the Kinesin movement can be classified into 3 states: resting, forward processive movement and detach/attachment to the MT. Once a Kinesin leaves the box from the vertical boundaries at $y = \pm \frac{L_y}{2}$ its corresponding image re enters from the opposite side. Those Kinesins which leave the last site in the x - direction at $i = L_x$ re enter into the MT from the left site $i = 1$.

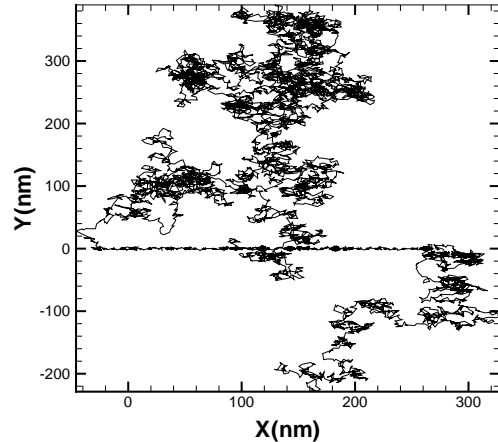


FIG. 5: 2D trajectory of a typical Kinesin at $\rho_g = 0.4$. Its corresponding space-time plot is sketched in Fig.7.

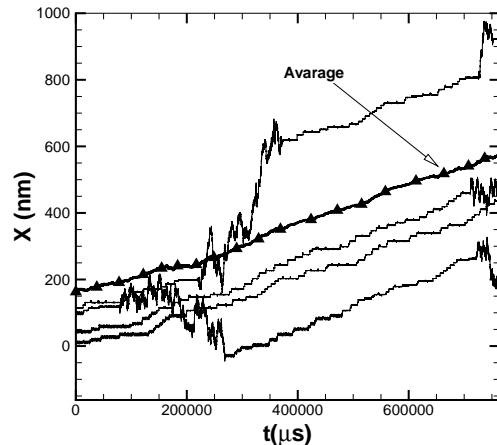


FIG. 6: Space-time plots of some Kinesins and the time dependence of their centre of mass at $\rho_g = 0.4$. Despite each Kinesin undergoes rapid fluctuations upon becoming unbound, the centre of mass (CM) has a smooth increasing behaviour.

Figure (5) exhibits the trajectory of a typical Kinesin at the global density $\rho_g = 0.4$:

Figure (6) exhibits the space-time plots of some more Kinesins and the time dependence of their centre of mass at $\rho_g = 0.4$. We observe that although each Kinesin undergoes rapid fluctuations upon becoming unbound, the centre of mass (CM) has a smooth increasing behaviour in time. We have found the CM velocity by fitting a linear line to the the curve as $v_{cm} = 0.5 \mu m/s$. As can be seen, when a Kinesin is attached to the MT, its x component undergoes small fluctuations and is frequently increasing with time. It rarely undergoes backward motion which is consistent with in-vitro experiments [8, 41, 42].

On the occasion of detachment from the MT, the Ki-

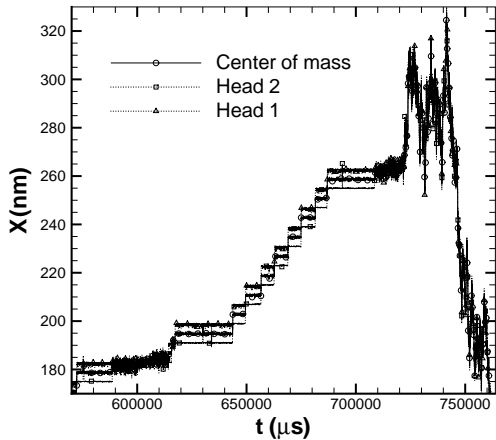


FIG. 7: Processive motion of a Kinesin along the MT.

nesin performs a stochastic random motion, in the cytoplasmic environment, which is characterized by large fluctuations. It is a well-known fact that Kinesins are processive motors i.e., they can move directedly along the filament for relatively large distances before detaching from it. Our model can successfully reproduce this behaviour in the collective motion of Kinesins. To illustrate this behaviour, we have explicitly shown x component time dependence of the two heads as well as the centre of mass for a typical Kinesin in the following figure.

As can be seen from Figure (7), the hand-over-hand mechanism of the directed motion is evident. In order to find a better insight, we have evaluated the dependence of a single Kinesin mean squared displacement (MSD) on time. The MSD has been obtained by averaging over the trajectories of all the Kinesins. Figure (8) depicts the time behaviour of a single Kinesin' MSD for various global Kinesin concentration ρ_g in a log-log plot.

We have evaluated the slopes by linear curve fitting. To a very good approximation the diffusion is normal for densities larger than $\rho_g \sim 0.2$ i.e., the MSD grows linearly in time. It would be more appropriate to define a line density ρ . This quantity is defined as the time average number of bound Kinesins to the MT. Note that a bound Kinesin can occupy two or one site of the MT depending on whether one or two heads are attached. We have sketched the dependence of ρ on ρ_g in Figure (9).

We observe a linear increase of ρ up to $\rho_g = 0.4$. Afterwards the rate of increase is lowered. This is due strong repulsion between bound Kinesins. We stress that in order to have values of ρ larger than 0.6 we have to significantly increase ρ_g . This enormously rises the computational costs. We extrapolated the behaviour of the curve for larger ρ . It turns out that ρ tends to an asymptotic value near 0.7. More specifically, let us denote the number of those bound Kinesins attached via one head to MT by N_1 and those attached via two heads by N_2 so

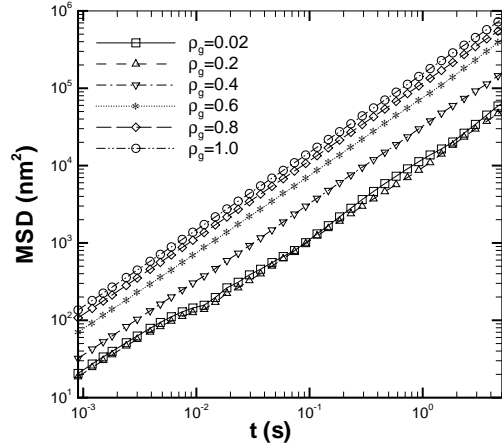


FIG. 8: Single Kinesin mean squared displacement versus time for various densities. To a very good approximation the diffusion is normal for densities larger than $\rho_g \sim 0.2$ i.e.; the MSD grows linearly in time.

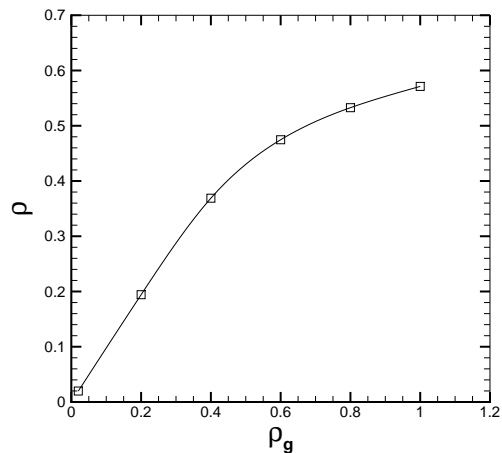


FIG. 9: Dependence of the line density ρ on the global density ρ_g . ρ tends to an asymptotic value near 0.7.

we have $N = N_0 + N_1 + N_2$ (N is the total number of Kinesins). Furthermore, we show the number unbound Kinesins by N_0 and the MT binding sites by N_{bs} .

$$\rho_g = \frac{N_0 + N_1 + N_2}{N_{bs}}; \quad \rho = \frac{N_1 + N_2}{N_{bs}} \quad (12)$$

In the extreme limit $\rho_g \rightarrow \infty$ we have (by extrapolation) $\rho = 0.7$, on the other hand we have $2N_2 + N_1 = N_{bs}$ which means all the sites are occupied by Kinesin heads. We therefore find that sixty percent of the sites are occupied by double-head attached Kinesins and forty percent by single-head attached Kinesins. In the following graphs, we exhibit the dependence of some cooperative

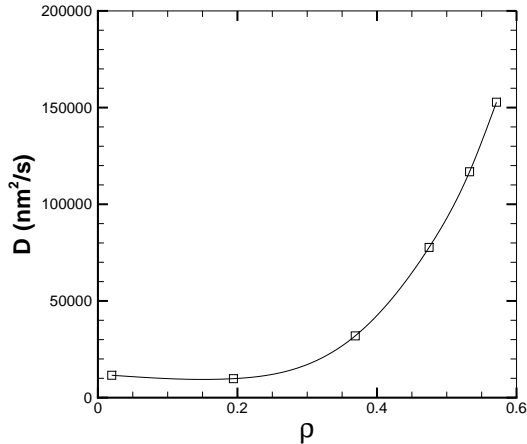


FIG. 10: Diffusion coefficient D of a single Kinesin versus density. The diffusion constant D turns out to be an increasing function of ρ . It grows slowly for small densities but shows a rapid increment for $\rho > 0.3$. The reason is due to increase of unbound Kinesins when the density is enhanced.

quantities on the line density ρ . In Figure (10) we exhibit the dependence of a single Kinesin diffusion coefficient D versus ρ . It grows slowly for small densities but shows a rapid increment for $\rho > 0.3$. The reason is due to increase of unbound Kinesins when the density is enhanced. Obviously, an unbound Kinesin performs a diffusive motion therefore increasing the number of unbound Kinesins gives rise to enhancement of the overall diffusion which in turn leads to a larger D . Note that D has been obtained by averaging over the trajectories of all the Kinesins.

We next turn into the issue of directed motion of Kinesins. First, we have computed the dependence of the averaged velocity of the CM versus ρ . Figure (11) sketches this behaviour.

To obtain the above graph, we plotted X_{cm} versus time and fitted a linear curve to it. The slope of the fitted line corresponds to the averaged velocity. As expected, $\langle V_x \rangle$ is a decreasing function of ρ . For small densities it decreases smoothly. However, when the density goes beyond $\rho = 0.2$, $\langle V_x \rangle$ shows a rapid decrease. In figure (12) we have exhibited the mean directed passage length (processive run length), the mean processive time and the velocity of this directed motion on the MT as a function of ρ .

The average processive run length \bar{L}_{prs} defined as the average distance a Kinesin can move processively on the MT before detachment exhibits a rapidly decreasing behaviour up to $\rho = 0.4$. After this value it shows a weak dependence on ρ . We speculate that at this density large traffic jams are formed which do not allow Kinesins to move directedly. The analogous behaviour is observed for the mean temporal processivity \bar{T}_{prs} . Dividing \bar{L}_{prs} by \bar{T}_{prs} gives us the average velocity \bar{V}_{prs} of the proces-

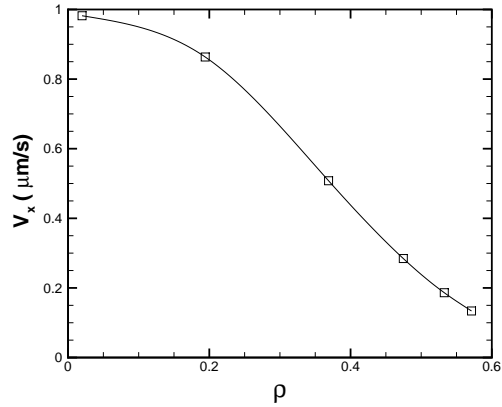


FIG. 11: Averaged CM velocity versus density ρ . $\langle V_x \rangle$ is a decreasing function of ρ . For small densities it decreases smoothly. When ρ goes beyond $\rho = 0.2$, $\langle V_x \rangle$ shows a rapid decrease.

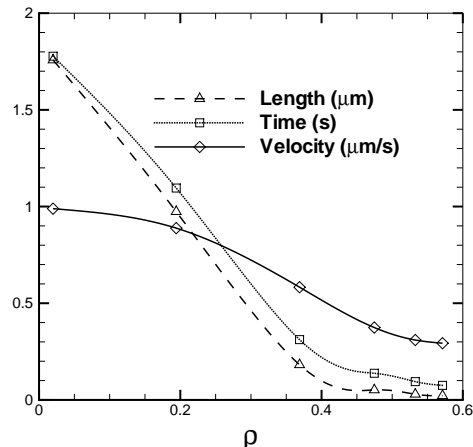


FIG. 12: Averaged directed processive run length, time and velocity versus density. Average processive run length exhibits a rapidly decreasing behaviour up to $\rho = 0.4$. After this value it shows a weak dependence on ρ . The analogous behaviour is observed for the mean temporal processivity.

sive motion. The average velocity has a more smooth decreasing behaviour. Having obtained the velocity of the directed motion, we are able to find the dependence of the current of Kinesins along the microtubule. The current J is defined by the fluid mechanics relation $J = \rho_g \bar{V}_{prs}$. Figure (13) sketches the dependence of J versus ρ .

J exhibits a maximum at $\rho \sim 0.34$. The interesting point is the existence of an asymmetry in the $J - \rho$ diagram. Normally in lattice driven gas models such as *asymmetric simple exclusion process* (ASEP) J appears as a symmetric function of ρ [43]. The current J is related to the rate of cargo transport by Kinesin motor proteins. In order to find a deeper understanding, we have

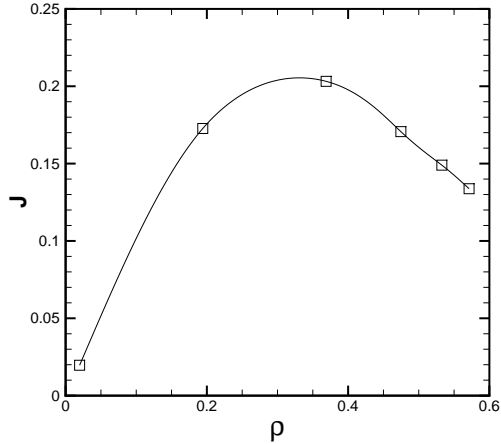


FIG. 13: Average Kinesins current versus density. It shows a maximum at $\rho \sim 0.34$.

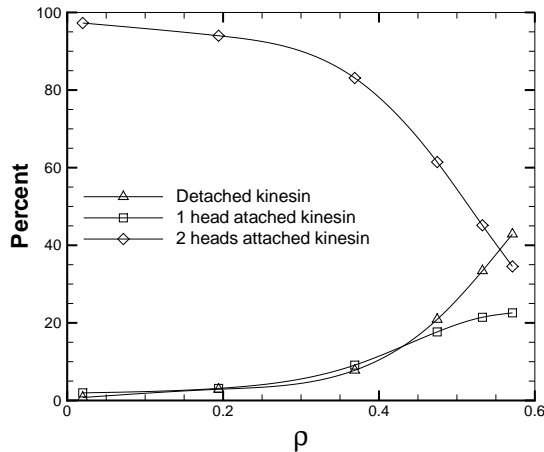


FIG. 14: Percentage of averaged bound and unbound Kinesins on the MT vs density.

evaluated the steady state percentage of the bound and unbound Kinesins as a function of ρ . Bound Kinesins are divided into two groups: one-head attached and two-head attached to the MT. Figure (14) exhibits this behaviour. Percentage of unbound Kinesins increases with density. In the same manner, percentage of one-head attached Kinesins increases with ρ but it seems to become saturated at large densities. Interestingly, percentage of two-head attached Kinesins shows a decreasing behaviour. The rate of decrease is small at low densities but becomes larger for higher densities.

IV. SUMMARY AND CONCLUDING REMARKS

We have simulated the collective motion of Kinesins on a microtubular track by developing a two dimensional Langevin-type model. The model is capable of reproducing the hand-over-hand mechanism of the directed motion along the microtubule. Various quantities such as diffusion constant, average velocity and the number current of Kinesins have been obtained by performing extensive molecular dynamics simulations. Dependence of the above quantities on the overall density of Kinesins have been obtained. It is shown that beyond a certain density, the average velocity and the current undergo notable decrease which is due to formation of traffic jams in the system. This observation is in accord to the ubiquitous flow-density characteristics.

-
- [1] J. Howard and R. L. Clark, *Applied Mechanics Reviews* **55**, B39 (2002).
 - [2] M. Schliwa, *Molecular Motors* (Wiley-VCH, 2003).
 - [3] M. Schliwa and G. Wöhlke, *Nature* **422**, 759 (2003).
 - [4] F. Jlicher, A. Ajdari, and J. Prost, *Reviews of Modern Physics* **69**, 1269 (1997).
 - [5] D. Chowdhury, K. Nishiniri, L. Santen, and A. Schadschneider, Elsevier (2008).
 - [6] F. J. Nédélec, T. Surrey, A. C. Maggs, and S. Leibler, *Nature* **389**, 305 (1997).
 - [7] F. Ndlec, T. Surrey, and E. Karsenti, *Current Opinion in Cell Biology* **15**, 118 (2003).
 - [8] M. J. Schnitzer and S. M. Block, *Nature* **227**, 386 (1997).
 - [9] Y. Okada and N. Hirokawa, *Science* **283**, 1152 (1999).
 - [10] J. Howard, A. J. Hudspeth, and R. D. Vale, *Nature* **342**, 154 (1989).
 - [11] S. M. Block, L. S. B. Goldstein, and B. J. Schnapp, *Nature* **348**, 348 (1990).
 - [12] D. D. Hackney, *Nature* **377**, 448 (1995).
 - [13] W. Hua, J. Chung, and J. Gelles, *Science* **295**, 844 (2002).
 - [14] A. Yildiz and P. R. Selvin, *Trends in Cell Biology* **15**, 112 (2005).
 - [15] J. Howard, *Annu Rev Physiol* **58**, 703 (1996).
 - [16] R. Lipowsky, S. Klumpp, and T. M. Nieuwenhuizen, *Phys Rev Lett* **87**, 108101 (2001).
 - [17] S. Klumpp and R. Lipowsky, *Journal of Statistical Physics* **113**, 233 (2003).
 - [18] S. Klumpp and R. Lipowsky, *Europhysics Letters* **66**, 90 (2004).

- [19] S. Klumpp, T. M. Nieuwenhuizen, and R. Lipowsky, *Biophys J* **88**, 3118 (2005).
- [20] R. Lipowsky and S. Klumpp, *Physica A: Statistical Mechanics and its Applications* **352**, 53 (2005).
- [21] A. B. Kolomeisky and H. Phillips, *J. Phys.: Condens. Matter* **17**, S3887 (2005).
- [22] A. Parmeggiani, T. Franosch, and E. Frey, *Physical Review E* **70**, 46101 (2004).
- [23] A. Ajdari, *J. Phys. I France*, **4**, 1577 (1994).
- [24] I. Deryni and T. Vicsek, *Proceedings of the National Academy of Sciences of the United States of America* **93**, 6775 (1996).
- [25] A. B. Kolomeisky and B. Widom, *Journal of Statistical Physics* **93**, 633 (1998).
- [26] S. Klumpp, A. Mielke and C. Wald, *Phys. Rev. E* **63**, 031914 (2001).
- [27] D. Dan, A. M. Jayannavar, and G. I. Menon, *Physica A: Statistical Mechanics and its Applications* **318**, 40 (2003).
- [28] X. Ping, D. Shuo-Xing, and W. Peng-Ye, *Chinese Physics* **13**, 1569 (2004).
- [29] J. L. Mateos, *Physica A: Statistical Mechanics and its Applications* **351**, 79 (2005).
- [30] Y. Jamali, A. Lohrasebi, and H. Rafii-Tabar, *Physica A: Statistical Mechanics and its Applications* **381**, 239 (2007).
- [31] K. Nishinari, Y. Okada, A. Schadschneider, and D. Chowdhury, *Arxiv preprint physics/0506014* (2005).
- [32] J. M. Scholey, J. Heuser, J. T. Yang, and L. S. B. Goldstein, *Nature* **338**, 355 (1989).
- [33] R. D. Vale and R. A. Milligan, *Science* **288**, 88 (2000).
- [34] N. J. Carter and R. A. Cross, *Nature* **435**, 308 (2005).
- [35] C. L. Asbury, A. N. Fehr, and S. M. Block, *American Association for the Advancement of Science*, (2003), Vol. 302, p. 2130.
- [36] S. P. Gilbert, M. R. Webb, M. Brune, and K. A. Johnson, *Nature* **373**, 671 (1995).
- [37] S. P. Gilbert and K. A. Johnson, *Biochemistry* **33**, 1951 (1994).
- [38] Y. Z. Ma and E. W. Taylor, *J Biol Chem* **272**, 717 (1997).
- [39] R. A. Cross, *Trends in Biochemical Sciences* **29**, 301 (2004).
- [40] E. P. Sablin and R. J. Fletterick, *Journal of Biological Chemistry* **279**, 15707 (2004).
- [41] M. Nishiyama, H. Higuchi, and T. Yanagida, *Nature Cell Biology* **4**, 790 (2002).
- [42] H. Kojima, E. Muto, H. Higuchi, and T. Yanagida, *Biophysical Journal* **73**, 2012 (1997).
- [43] G. Schütz in: *Phase transitions and Critical Phenomena, vol 19*, ed. C. Domb and L. Lebowitz, Academic Press, 2001.